

Mutual information in heavy-fermion systems

Francesco Parisen Toldin,^{*} Toshihiro Sato,[†] and Fakher F. Assaad[‡]

Institut für Theoretische Physik und Astrophysik, Universität Würzburg, Am Hubland, 97074 Würzburg, Germany

A key notion in heavy-fermion systems is the entanglement between conduction electrons and localized spin degrees of freedom. To study these systems from this point of view, we compute the mutual information in a ferromagnetic and antiferromagnetic Kondo lattice model in the presence of geometrical frustration. Here the interplay between the Kondo effect, the Ruderman-Kittel-Kasuya-Yosida interaction, and geometrical frustration leads to partial Kondo screened, conventional Kondo insulating, and antiferromagnetic phases. In each of these states the mutual information follows an area law, the coefficient of which shows sharp crossovers (on our finite lattices) across phase transitions. Deep in the respective phases, the area law coefficient can be understood in terms of simple direct product wave functions thereby yielding an accurate measure of the entanglement in each phase. The above-mentioned results stem from approximation-free auxiliary field quantum Monte Carlo simulations.

I. INTRODUCTION

The Kondo effect describes the screening of a spin-1/2 magnetic impurity embedded in a metallic environment [1]. At high temperatures the spin degree of freedom is decoupled from the conduction electrons and below the Kondo scale a many body entangled state of the spin and conduction electrons emerges. To quantify entanglement between a bipartition A and B of a system, one traces out the degrees of freedom B to obtain a reduced density matrix, $\hat{\rho}_A = \text{Tr}_{\mathcal{H}_B} \hat{\rho}$, the Renyi entropy of which, $S_n(A) = (\ln \text{Tr} \hat{\rho}_A^n) / (1 - n)$, corresponds to the entanglement entropy. Taking one subsystem to be the impurity spin, and the other the conduction electrons, the Kondo effect can be elegantly characterized by the transfer of $\ln(2)$ thermal entropy at high temperatures to $\ln(2)$ entanglement entropy in the ground state, as recently computed in a Kondo impurity model [2] and in a spin-1/2 chain sharing the same low-energy behavior [3]. The energy scale at which this transfer from the thermal entropy to the entanglement entropy occurs is the Kondo temperature. More generally, local entanglement is an important feature of two-level dissipative systems [4, 5].

In the presence of a lattice of spins Kondo coupled to conduction electrons, corresponding to heavy-fermion systems [6], the above picture breaks down. In fact spins can now interact through the indirect Ruderman-Kittel-Kasuya-Yosida (RKKY) exchange interaction [7], and thereby compete with Kondo screening. Comparing these two energy scales, it becomes apparent that Kondo screening dominates when the exchange interaction between the localized spins and the conduction electrons, J_K , is positive and large, and that the RKKY interaction dominates at small values of J_K . The intricate interplay between these two effects on nonfrustrated lattices leads to a quantum phase transition (QPT) between disordered and ordered magnetic phases [8–11]. The Kondo effect can be switched off by considering $J_K < 0$, thereby promoting magnetically ordered phases [12]. In ad-

dition, geometrical frustration is found to be of experimental relevance in many heavy-fermion materials such as CePdAl, Pr₂Ir₂O₇, YbAgGe, YbAl₃C₃, Yb₂Pt₂Pb [13–17], where quantum phases do not easily fit into the aforementioned cases. Geometrical frustration can lead to so-called partial Kondo screened (PKS) phases where frustration is alleviated by selective spatial screening localized spins [18–22]. The essence of all aforementioned states can be captured by direct product variational wave functions from which one can directly assess the degree of entanglement between the spins and conduction electrons. Entanglement entropies, although not presently experimentally accessible in heavy-fermion systems, lend themselves to an experimental measure in systems of cold atoms [23], which, in turn, allow one to realize Kondo lattice models [24]. Alternatively, entanglement properties have been recently proposed to be experimentally studied by engineering the so-called entanglement Hamiltonian in cold atom systems [25]. In this context, Ref. [26] introduces a numerically exact method to determine the entanglement Hamiltonian in interacting models of fermions.

In this paper we investigate a Kondo lattice model Hamiltonian amenable to negative-sign-free quantum Monte Carlo (QMC) simulations that provide specific realizations of the states discussed above. Using recently developed methods to compute the Renyi entropies [27] with the auxiliary field QMC, we compute the mutual information and show that, deep in the respective phases, the numerical value of the area law coefficient can be well understood in terms of the product state wave function description of the phase supplemented by fluctuations, if necessary. Furthermore, we observe a singular behavior of the area law coefficient across phase transitions.

II. MODEL

We consider the generalized Kondo lattice model on the honeycomb lattice introduced in [22] with Hamiltonian

$$\hat{H} = -t \sum_{\langle i,j \rangle} \hat{c}_i^\dagger \hat{c}_j + J_K \sum_i \frac{1}{2} \hat{c}_i^\dagger \boldsymbol{\sigma} \hat{c}_i \cdot \hat{\mathbf{S}}_i + J_z \sum_{\langle\langle i,j \rangle\rangle} \hat{S}_i^z \hat{S}_j^z \quad (1)$$

where the first sum extends over the nearest-neighbor sites and describes the hopping of conduction electrons, $\hat{c}_i^\dagger =$

^{*} francesco.parisentoldin@physik.uni-wuerzburg.de

[†] Toshihiro.Sato@physik.uni-wuerzburg.de

[‡] assaad@physik.uni-wuerzburg.de

$(\hat{c}_{i,\uparrow}^\dagger, \hat{c}_{i,\downarrow}^\dagger)$, giving rise to the well-known semimetallic band dispersion [28], the second sum accounts for the Kondo screening interaction between conduction electrons and spin-1/2 local moments \hat{S}_i , while the third term is the next-nearest-neighbor antiferromagnetic interaction between localized spins encodes frustration effects. This model can be solved without encountering the negative sign problem [22]; here and in the following we consider half-filling for the conduction electron and use $t = 1$ as the energy unit. Due to the antiferromagnetic coupling J_z this half-filled Kondo lattice model on the honeycomb lattice with geometric frustration exhibits PKS phases alongside the conventional Kondo insulator (KI) and antiferromagnetically ordered phases [22].

The mutual information $I_n(\Gamma_c, \Gamma_S)$ between two subsystems of conduction electrons Γ_c and of localized spins Γ_S is

$$I_n(\Gamma_c, \Gamma_S) \equiv S_n(\Gamma_c) + S_n(\Gamma_S) - S_n(\Gamma_c \cup \Gamma_S), \quad (2)$$

where $S_n(\Gamma)$ is the n th Renyi entropy for a subsystem Γ . Here we take Γ_c as a compact subset of N conduction electron sites, and Γ_S as the corresponding N localized spin sites coupled to the subset Γ_c . Assuming the ubiquitous area law for the entanglement entropy [29], $I_n(\Gamma_c, \Gamma_S)$ results are proportional to the size of the boundary shared between Γ_c and Γ_S :

$$I_n(\Gamma_c, \Gamma_S) \simeq \alpha 2N. \quad (3)$$

The mutual information is also defined in terms of the von Neumann entanglement entropy, corresponding to the limit $n \rightarrow 1$ in Eq. (2). In this case $I_1(\Gamma_c, \Gamma_S)$ satisfies [30]

$$I_1(\Gamma_c, \Gamma_S) \geq \frac{\langle O_c O_S \rangle - \langle O_c \rangle \langle O_S \rangle}{\|O_c\|^2 \|O_S\|^2}, \quad (4)$$

where the numerator represents the connected correlation of two arbitrary operators O_c and O_S acting on the subsystem Γ_c and Γ_S , respectively, and $\|X\| \equiv \{\sup \sqrt{\langle \psi | X^\dagger X | \psi \rangle}, \langle \psi | \psi \rangle = 1\}$ is the norm of an operator X . According to Eq. (4), $I_1(\Gamma_c, \Gamma_S)$ bounds all mutual correlations of operators in Γ_c and Γ_S , thus providing an operator-independent entanglement measure. Due to the above bound, $I_1(\Gamma_c, \Gamma_S)$ captures both high- and low-energy scales.

Here, we shall consider the mutual information for Renyi index $n = 2$. The coefficient α introduced in Eq. (3) is the main quantity investigated in this work. In the presence of Kondo screening $I_n(\Gamma_c, \Gamma_S)$ essentially counts the number of Kondo singlets formed between Γ_c and Γ_S , such that in the limit $J_K \rightarrow \infty$ Eq. (3) holds exactly with $\alpha = \ln(2)$.

III. METHOD

We have investigated the Hamiltonian of Eq. (1) by means of auxiliary field QMC [31–33] simulations, using the method of Ref. [22] which, in essence, consists in a fermion representation of localized spins obtained via Lagrange multipliers. We refer to Ref. [22] for more details on the formulation. A similar technique can be used to simulate the canonical ensemble [34]. Simulations have been performed using

the ALF package [35]. To compute the Renyi entropies we have used a method introduced in Ref. [27], and also used in [36–39], which allows to formulate the reduced density matrix within auxiliary field QMC. Beside Renyi entropies, the technique can be exploited to unbiasedly determine the entanglement Hamiltonian [26]. Reference [40] provides a short review of computational approaches to entanglement in interacting fermionic systems.

IV. RESULTS

In Fig. 1(a) we reproduce the rich phase diagram of the model for $J_K > 0$, $J_z \geq 0$. At finite J_z the model has a reduced U(1) spin symmetry corresponding to spin rotations around the z axis, as well as the point group and translation symmetries of the honeycomb lattice. The KI phase breaks no symmetries, the in-plane antiferromagnetic (xy -AFM) phase breaks the U(1) spin symmetry, and the z -PKS phase breaks nematically the point group and has reduced translation symmetry. The xyz -PKS phase differs from the z -PKS one in that it additionally breaks the U(1) spin symmetry [22]. In Fig. 1(a) we also show three lines on the phase diagram where we analyze the mutual information. Moreover, we study the entanglement for $J_K < 0$, $J_z = 0$, where the model favors the formation of an effective spin $S = 1$ Heisenberg antiferromagnet in the strong-coupling limit. In all the QMC data presented here we have simulated a lattice 6×6 unit cells corresponding to 144 orbitals.

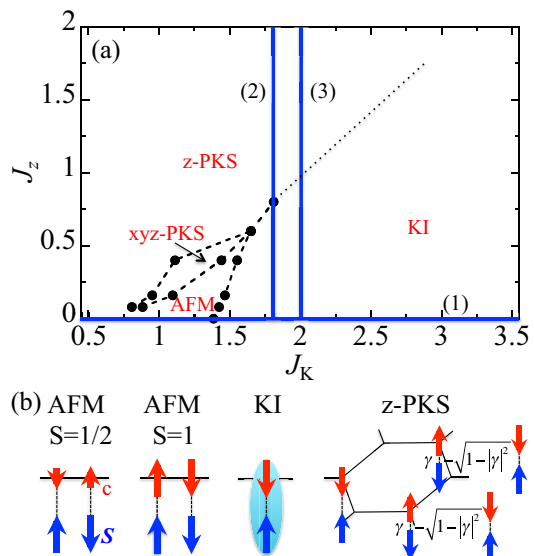


FIG. 1. (a) Ground-state phase diagram with antiferromagnetic (AFM), out-of-plane PKS (z -PKS), spin-rotation symmetry breaking PKS (xyz -PKS), and KI phases from QMC simulations [22]. Dashed lines connects transition points and the dotted line sketches the expected boundary between the KI and z -PKS phases. The three thick lines indicate the scans of the phase diagram considered here. (b) Mean-field schematic picture of $S = 1/2$ and $S = 1$ AFM, KI, and z -PKS phases.

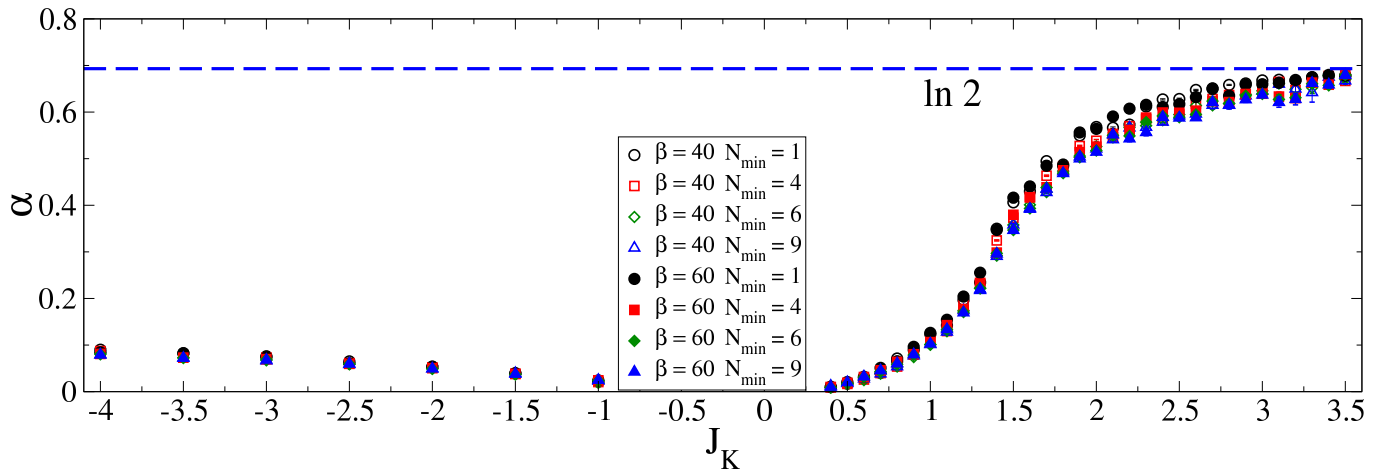


FIG. 2. Coefficient α of the area law for the mutual information along the line (1) on Fig. 1(a) and also for $J_K \leq -1$, $J_z = 0$. We consider two inverse temperatures $\beta = 40, 60$, and for four values of the minimum subsystem size taken into account in the fits.

We first consider a scan for $J_z = 0$, where the model reduces to a standard Kondo lattice model on the honeycomb lattice with the conventional RKKY driven AFM phase and KI phase. A fit of $I_2(\Gamma_c, \Gamma_S)$ for up to nine choices of Γ_c, Γ_S to the right-hand side of Eq. (3) allows us to extract the coefficient α shown in Fig. 2, for two inverse temperatures $\beta = 40, 60$, and as a function of the minimum subsystem size N_{\min} taken into account in the fits. More technical details on the chosen subsystems Γ_c, Γ_S are reported in Appendix A. We observe consistent results for the fitted values of α . In the KI phase conduction and localized electrons are paired into a spin singlet, such that for $J_K \gg 0$ the ground state approaches a product of single-site singlet wave functions shown in Fig. 1(b), giving a $\ln(2)$ entanglement entropy per pair. Indeed, in the KI phase α reaches an asymptotic value $\ln(2)$ for $J_K \gtrsim 3$. Interestingly, a change of concavity in the plot of α occurs around the QPT between the AFM and KI phases, at $J_K \simeq 1.4$ [22]. In the AFM phase at $J_K > 0$ the conduction electron local moment aligns antiparallel to the spin and is reduced in magnitude due to charge fluctuations. The essential features of the AFM phase can be captured by a product wave function, in which the total local moment of conduction electrons and spins form a Néel order as depicted in Fig. 1(b). Entanglement between spins and conduction electrons originates from subleading Kondo screening as argued in Ref. [12] and also from long-wavelength spin-wave fluctuations of the Néel order parameter. In Fig. 2 we also show α for a ferromagnetic coupling $J_K < 0$. Different than the $J_K > 0$ case, here the Kondo coupling favors the formation of a spin triplet in the ground state of the model, without Kondo screening. Starting from the limit $J_K \rightarrow -\infty$, where on each lattice site the spin singlet state $|S = 0\rangle$ is projected away, a finite large value of $J_K < 0$ gives rise to an antiferromagnetic exchange term between $S = 1$ states on the honeycomb lattice. Thus, in this situation the system reduces to a Heisenberg $S = 1$ model. Its antiferromagnetic ground state is well captured by the semiclassical large- S expansion, and consists in a Néel state, illustrated in Fig. 1(b). Since such a ground state is pri-

marily built on $|S = 1, S_z = \pm 1\rangle$ states, the entanglement between conduction electrons and localized spins is expected to be small. This observation is clearly reflected in the α coefficient shown in Fig. 2, whose values for $J_K < 0$ are substantially smaller than for $J_K > 0$. For instance, we find $\alpha \simeq 0.1$ for $J_K = 1$ and $\alpha \simeq 0.024$ for $J_K = -1$. The computed value of α grows on reducing $J_K < 0$, but appears to saturate to a value significantly smaller than the limiting value $\ln(2)$ found for $J_K \rightarrow \infty$.

In order to investigate the z -PKS phase we compute the mutual information as a function of J_z for fixed $J_K = 1.8$. As illustrated in Fig. 1(a), this second scan crosses the conventional KI and z -PKS phases. Due to an enlarged unit cell expected in the z -PKS phase [22], we have in this case considered only three possible subsystems Γ_c, Γ_S , with equal size $N = 6, 13, 22$. In view of the limited amount of available data, and in order to reliably study the coefficient α we have considered three possible linear fits: a fit including all data, a fit disregarding the smallest size $N = 6$, and a fit disregarding the largest size $N = 22$. In Fig. 3(a) we show the corresponding results, for two inverse temperatures $\beta = 30, 40$. Despite fluctuations larger than the error bars, indicating sizable corrections to Eq. (3), we observe a clear trend in α , which decreases from $\alpha \approx 0.45$ to $\alpha \approx 0.17$. Moreover, the curve shows again a change in the curvature at a value of J_z approximately consistent with the onset of a QPT between the KI and z -PKS phases, located at $J_z \approx 0.8$ [22] [see also Fig. 1(a)]. For $J_z \gtrsim 1.4$, α saturates to a plateau $\alpha \approx 0.17$. Such a value, which approaches the limit $J_z \rightarrow \infty$ at fixed J_K is in fact J_K -dependent, as shown by the computation of α along path (3) in Fig. 1(a). In Fig. 3(b) we show the resulting α , whose curves are qualitatively similar to the case of Fig. 3(a), but saturate to a large value $\alpha \approx 0.23$ for large J_z .

The emergence of an area law with a coefficient $\alpha < \ln(2)$ confirms the mechanism of partial Kondo screening in the z -PKS phase, emerging from the competition of the antiferromagnetic interaction and the Kondo coupling. To understand the structure of the ground state we consider the limit

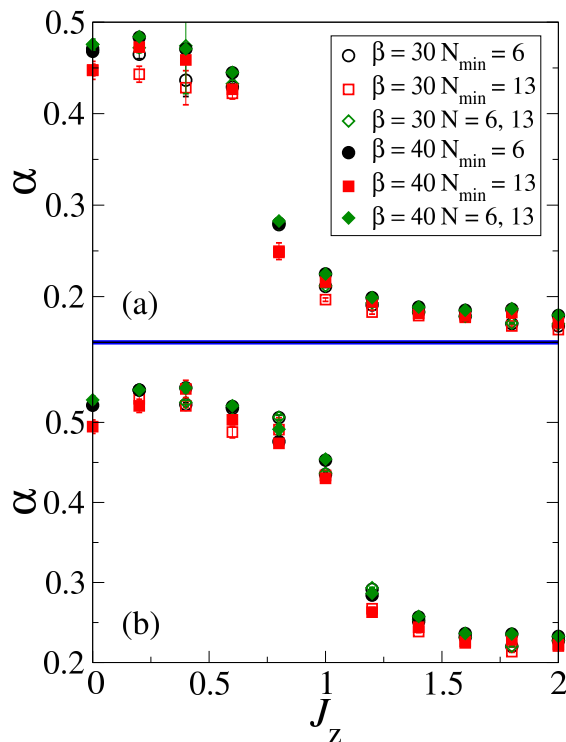


FIG. 3. Coefficient α of the area law for the mutual information along line (2) (above) and line (3) (below) on Fig. 1(a), for inverse temperatures $\beta = 30, 40$, and three different fits (see main text).

$J_K, J_z \rightarrow \infty$, i.e., the atomic limit $t = 0$ in which the honeycomb lattice decomposes into two independent triangular sublattices. In this limit the Hamiltonian (1) commutes with the z component of the total spin operator on site i , $S_i^{\text{tot},z} \equiv S_i^{c,z} + S_i^z$, with $S_i^{c,z} \equiv (1/2)\hat{c}_i^\dagger \sigma_z \hat{c}_i$. Accordingly, one expects the ground state to have $S_i^{\text{tot},z} = 0$, such that its wave function is constructed from the states $|+\rangle_i \equiv |\uparrow, \downarrow\rangle_i$ and $|-\rangle_i \equiv |\downarrow, \uparrow\rangle_i$, whereas states obtained with the remaining base vectors $|\uparrow, \uparrow\rangle_i$ and $|\downarrow, \downarrow\rangle_i$ are gapped. In the Hilbert space spanned by $\{|+\rangle_i, |-\rangle_i\}$ the Hamiltonian (1) is, up to a constant,

$$\hat{H} = \frac{J_z}{4} \sum_{\langle\langle i,j \rangle\rangle} \hat{Z}_i \hat{Z}_j + \frac{J_K}{2} \sum_i \hat{X}_i + \dots, \quad (5)$$

where the operators \hat{Z}_i, \hat{X}_i are defined by $\hat{Z}_i|\pm\rangle_i = \pm|\pm\rangle_i$, $\hat{X}_i|\pm\rangle_i = |\mp\rangle_i$ and satisfy the commutation rule of the SU(2) algebra. Therefore, in the atomic limit and close to the ground state the Hamiltonian (1) reduces to that of an antiferromagnetic transverse-field Ising model, on a triangular lattice. Beyond the atomic limit, the effective low-temperature Hamiltonian acquires additional interactions which we have already anticipated in Eq. (5). However since for a finite, but large, J_K/t , and still $J_K \ll J_z$ the additional states are gapped, we expect the ground state to be well representable in the $\{|+\rangle_i, |-\rangle_i\}$ basis. It is known that the above Ising model has a three sublattice structure and that the sign of the sixfold clock term in the Landau-Ginzburg functional determines if

the ground state will be hierarchical, $|\Psi\rangle = |+\rangle_i |-\rangle_j (|+\rangle_k + |-\rangle_k)/\sqrt{2}$, or uniform [41, 42],

$$|\Psi\rangle = |+\rangle_i \left(\gamma |+\rangle_j - \sqrt{1-|\gamma|^2} |-\rangle_j \right) \otimes \left(\gamma |+\rangle_k - \sqrt{1-|\gamma|^2} |-\rangle_k \right). \quad (6)$$

Here, i, j, k label the three sites of the sublattice structure. Numerical calculations in Ref. [22] point to the uniform ground state, so we use this product wave function to account for our mutual information results. Here, $|\gamma| \leq 1$ controls the partial polarization of the sites j and k and the direct product wave function is illustrated in Fig. 1(b). As we discuss in Appendix B, for the state of Eq. (6), $\alpha = -(2/3) \ln(1 - 2|\gamma|^2 + 2|\gamma|^4)$, which takes values between 0 and $2 \ln(2)/3 \simeq 0.46$, thus including the plateaus found in Fig. 3.

V. CONCLUSIONS AND DISCUSSION

The bound on the von Neumann entanglement entropy based mutual information presented in Eq. (4) implies that for our choice of Γ_c and Γ_S the mutual information picks up IR as well as UV physics. Deep in a phase, or in a sink in the renormalization-group parlance, where the correlation length is finite one can model the ground state with a direct product wave function that provides a modeling of all energy scales. With this wave function the coefficient of the area law of the mutual information can be computed. In the Kondo lattice model considered here, we have an explicit realization of three phases, AFM, PKS, and KI. The simple direct product wave functions for these three phases presented in Fig. 1(b) have an area law coefficient set by $\alpha = 0$ for the Néel representation of the AFM phase, $\alpha = \ln(2)$ for the strong-coupling KI phase, and α bounded by $2 \ln(2)/3$ for the PKS phase. The KI value of α is exact in the strong J_K limit and is very well reproduced when J_K is comparable to half the bandwidth, $W = 6$. Deep in the PKS phase α shows a J_K dependent plateau upon enhancing J_z . The value of this plateau depends on the degree of partial Kondo screening as described by γ in Eq. (6). Clearly, the Néel wave function shows no entanglement, but of course does not capture fluctuations leading to Goldstone modes and to entanglement. For these phases, both for positive and negative values of J_K the mutual information remains *small* but does not vanish. It is however noticeable that α is larger in the AFM phase at $J_K > 0$ than at $J_K < 0$. We understand this difference in terms of subleading Kondo screening present for the antiferromagnetic model but absent for the ferromagnetic one. Computations of the single-particle spectral function [12] confirm this point of view.

On our finite lattices we have observed clear crossovers in the area law coefficient of the mutual information across phase transitions. How this behavior reflects the criticality of the transition as well as possible corrections to the area law at critical points is left to future investigations.

From the technical point of view, the present calculation of the mutual information does not lead to a noticeable increase

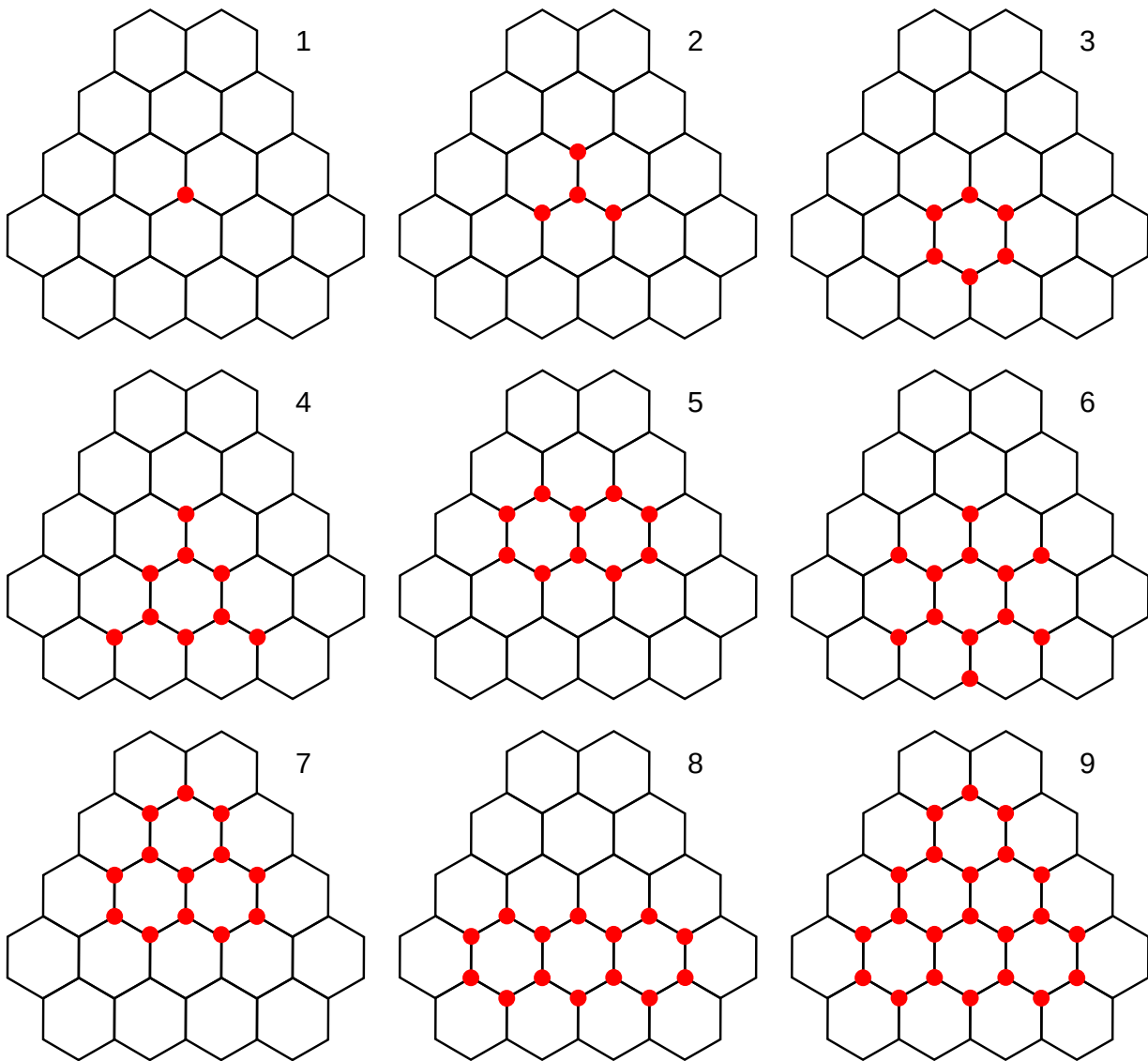


FIG. 4. Partition of lattice sites used to compute the mutual information $I_2(\Gamma_c, \Gamma_S)$. For each illustrated subset of sites, Γ_c is the corresponding set of conduction electron sites, and Γ_S the set of localized spin sites coupled to Γ_c . When $J_z > 0$, due to the enlarged unit cell we have computed $I_2(\Gamma_c, \Gamma_S)$ using only subsystems no. 3, no. 7, and no. 9.

in computational effort. It can be used as a standard *observable independent* measure to pick up QPTs and thereby map out phase diagrams in various heavy-fermion systems and beyond. This is very similar to unsupervised machine learning algorithms aiming at automatically mapping out phase diagrams [43]. As mentioned above it also provides further information on phases. In this context we note that this quantity has recently been used [44] to validate the understanding of a Kondo breakdown transition.

ACKNOWLEDGMENTS

We would like to thank T. Grover and J. S. Hofmann for insightful discussions. F.P.T. thanks the German Research Foundation (DFG) through Grant No. AS120/13-1 of the FOR

1807. T.S. thanks the DFG for financial support from Grant No. AS120/14-1. F.F.A. thanks the DFG through SFB 1170 ToCoTronics. We gratefully acknowledge the Gauss Centre for Supercomputing (GCS) under the project pr53ju for allocation of CPU time on the SuperMUC computer at the Leibniz Supercomputing Center.

APPENDIX A: COMPUTATION OF THE MUTUAL INFORMATION

In order to compute the coefficient α introduced in Eq. (3) we have sampled $I_2(\Gamma_c, \Gamma_S)$ choosing different subsets of lattice sites. As explained in the main text, Γ_c is a compact subset of lattice sites of the conduction electrons and Γ_S contains the localized spin sites coupled to Γ_c . In Fig. 4 we illustrate

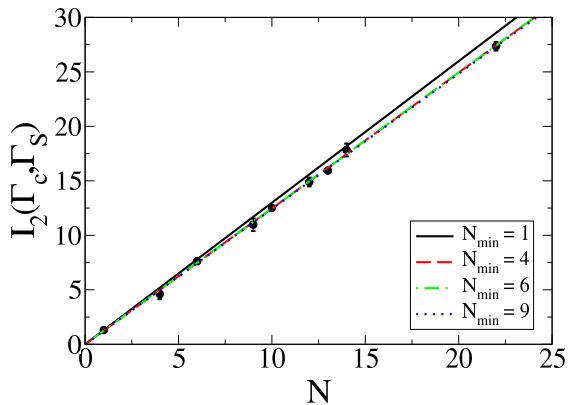


FIG. 5. Mutual information $I_2(\Gamma_c, \Gamma_S)$ at $J_K = 2.7$, $J_z = 0$, $\beta = 60$ for the choices of Γ_c , Γ_S shown in Fig. 4, as a function of the size N of Γ_c and Γ_S . We compare with a linear fit to the right-hand side of Eq. (3), for different choices of the minimum subsystem size N_{\min} taken into account.

the nine choices of Γ_c , Γ_S used here. In the presence of non-vanishing antiferromagnetic coupling J_z , due to the enlarged unit cell [22] we use only the subsystems no. 3, no. 7, and no. 9, shown in Fig. 4. As we discuss in the main text, for a given value of J_K and J_z , the coefficient α has been obtained by a linear fit of $I_2(\Gamma_c, \Gamma_S)$ as a function of the size N . In Figs. 5 and 6 we show two examples of such a procedure, in the KI phase and in the z -PKS phase.

APPENDIX B: RENYI ENTROPIES IN THE Z -PKS PHASE

For a product wave function ansatz like that in Eq. (6), and for any choice of Γ_c and Γ_S , consisting in a set of N conduction electron sites and in the set of the corresponding coupled localized spin sites, the reduced density matrix of $\Gamma_c \cup \Gamma_S$ is a pure state. Hence, $S_n(\Gamma_c \cup \Gamma_S) = 0$ and $S_n(\Gamma_c) = S_n(\Gamma_S)$,

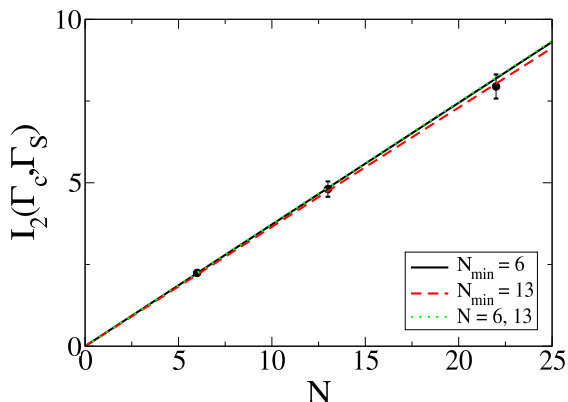


FIG. 6. Same as Fig. 5 for $J_K = 1.8$, $J_z = 1.8$, $\beta = 40$, in the z -PKS phase, and for subsystems no. 3, no. 7, and no. 9, shown in Fig. 4. We compare with three linear fits, obtained by using all data ($N_{\min} = 6$), disregarding the smallest size ($N_{\min} = 13$), and disregarding the largest size ($N = 6, 13$).

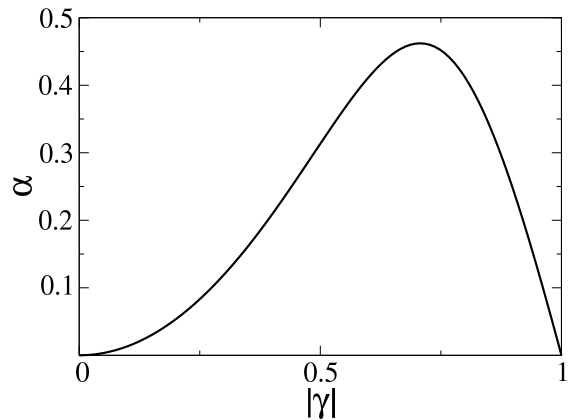


FIG. 7. Coefficient α of the mutual information area law for the wave function ansatz of Eq. (6).

such that, in order to determine $I_2(\Gamma_c, \Gamma_S)$ it is sufficient to compute the entanglement entropy of the localized spins $S_n(\Gamma_S)$. On each triangular unit cell, the ansatz of Eq. (6) results in a factorized reduced density matrix for Γ_S ,

$$\rho_S \equiv \text{Tr}_c |\Psi\rangle\langle\Psi| = \rho_i \rho_j \rho_k, \quad (\text{B1})$$

with $|\Psi\rangle$ as given in Eq. (6) and

$$\begin{aligned} \rho_i &= 1, \\ \rho_j &= \rho_k = \sum_{\sigma=\uparrow,\downarrow} \langle\sigma|\psi(\gamma)\rangle\langle\psi(\gamma)|\sigma\rangle, \\ |\psi(\gamma)\rangle &\equiv \gamma|+\rangle - \sqrt{1-|\gamma|^2}|-\rangle. \end{aligned} \quad (\text{B2})$$

Since, apart from a site index, the single-site reduced density matrices ρ_j and ρ_k are identical, in Eq. (B2) and in the following, with a slight abuse of notation, we have dropped the site indexes y, z in $|\psi(\gamma)\rangle$. Using the definition $|+\rangle \equiv |\uparrow, \downarrow\rangle$ and $|-\rangle \equiv |\downarrow, \uparrow\rangle$, the reduced density matrix for the sites j and k is readily computed as

$$\rho_j = \rho_k = (1-|\gamma|^2)|\downarrow\rangle\langle\downarrow| + |\gamma|^2|\uparrow\rangle\langle\uparrow|. \quad (\text{B3})$$

Using Eqs. (B2) and (B3) the second Renyi entropy for the single triangular unit cell is

$$S_2 = -2 \ln(1 - 2|\gamma|^2 + 2|\gamma|^4). \quad (\text{B4})$$

Finally, the coefficient α defined in Eq. (3) corresponding to the Renyi entropy of Eq. (B4) is

$$\alpha = -\frac{2}{3} \ln(1 - 2|\gamma|^2 + 2|\gamma|^4). \quad (\text{B5})$$

In Fig. 7 we plot α as a function of $|\gamma|$, for $|\gamma| \leq 1$. The minimum value of α is $\alpha = 0$, and corresponds to $\gamma = 0, 1$: for such values of γ the state is a product of a conduction electrons and a localized spins states. Viceversa, a maximum value of $\alpha = 2 \ln(2)/3$ is found for $\gamma = 1/\sqrt{2}$, corresponding to the maximally entangled spin singlet state.

- [1] A. C. Hewson, *The Kondo Problem to Heavy Fermions*, Cambridge Studies in Magnetism (Cambridge University Press, Cambridge, 1997).
- [2] C. Wagner, T. Chowdhury, J. H. Pixley, and K. Ingersent, Long-Range Entanglement near a Kondo-Destruction Quantum Critical Point, *Phys. Rev. Lett.* **121**, 147602 (2018).
- [3] E. S. Sørensen, M.-S. Chang, N. Laflorencie, and I. Affleck, Impurity entanglement entropy and the Kondo screening cloud, *J. Stat. Mech.* **L01001** (2007).
- [4] A. Kopp and K. Le Hur, Universal and Measurable Entanglement Entropy in the Spin-Boson Model, *Phys. Rev. Lett.* **98**, 220401 (2007).
- [5] K. Le Hur, Entanglement entropy, decoherence, and quantum phase transitions of a dissipative two-level system, *Annals of Physics* **323**, 2208 (2008).
- [6] P. Coleman, Heavy Fermions: Electrons at the Edge of Magnetism, in *Handbook of Magnetism and Advanced Magnetic Materials*, Vol. 1 (John Wiley and Sons, New York, 2007) pp. 95–148, [cond-mat/0612006](#).
- [7] C. Kittel, *Quantum Theory of Solids* (Wiley, New York, 1963).
- [8] S. Doniach, The Kondo lattice and weak antiferromagnetism, *Physica B* **91**, 231 (1977).
- [9] F. F. Assaad, Quantum monte carlo simulations of the half-filled two-dimensional kondo lattice model, *Phys. Rev. Lett.* **83**, 796 (1999).
- [10] H. V. Löhneysen, A. Rosch, M. Vojta, and P. Wölfle, Fermi-liquid instabilities at magnetic quantum phase transitions, *Rev. Mod. Phys.* **79**, 1015 (2007).
- [11] Q. Si, J. H. Pixley, E. Nica, S. J. Yamamoto, P. Goswami, R. Yu, and S. Kirchner, Kondo Destruction and Quantum Criticality in Kondo Lattice Systems, *J. Phys. Soc. Jap.* **83**, 061005 (2014).
- [12] S. Capponi and F. F. Assaad, Spin and charge dynamics of the ferromagnetic and antiferromagnetic two-dimensional half-filled Kondo lattice model, *Phys. Rev. B* **63**, 155114 (2001).
- [13] A. Sakai, S. Lucas, P. Gegenwart, O. Stockert, H. v. Löhneysen, and V. Fritsch, Signature of frustrated moments in quantum critical $\text{CePd}_{1-x}\text{Ni}_x\text{Al}$, *Phys. Rev. B* **94**, 220405(R) (2016).
- [14] S. Nakatsuji, Y. Machida, Y. Maeno, T. Tayama, T. Sakakibara, J. van Duijn, L. Balicas, J. N. Millican, R. T. Macaluso, and J. Y. Chan, Metallic Spin-Liquid Behavior of the Geometrically Frustrated Kondo Lattice $\text{Pr}_2\text{Ir}_2\text{O}_7$, *Phys. Rev. Lett.* **96**, 087204 (2006).
- [15] M. S. Kim, M. C. Bennett, and M. C. Aronson, $\text{Yb}_2\text{Pt}_2\text{Pb}$: Magnetic frustration in the Shastry-Sutherland lattice, *Phys. Rev. B* **77**, 144425 (2008).
- [16] K. Sengupta, M. K. Forthaus, H. Kubo, K. Katoh, K. Umeo, T. Takabatake, and M. M. Abd-Elmeguid, Geometrical frustration versus magnetic order in the heavy-fermion antiferromagnet YbAgGe under high pressure, *Phys. Rev. B* **81**, 125129 (2010).
- [17] Y. Kato, M. Kosaka, H. Nowatari, Y. Saiga, A. Yamada, T. Kobiyama, S. Katano, K. Ohoyama, H. S. Suzuki, N. Aso, and K. Iwasa, Spin-Singlet Ground State in the Two-Dimensional Frustrated Triangular Lattice: YbAl_3C_3 , *J. Phys. Soc. Jpn* **77**, 053701 (2008).
- [18] Y. Motome, K. Nakamikawa, Y. Yamaji, and M. Udagawa, Partial Kondo Screening in Frustrated Kondo Lattice Systems, *Phys. Rev. Lett.* **105**, 036403 (2010).
- [19] K. Noda, T. Yoshida, R. Peters, and N. Kawakami, Partial Kondo Screening in a Geometrically Frustrated Heavy Electron System, *JPS Conf. Proc.* **3**, 014019 (2014).
- [20] M. W. Aulbach, F. F. Assaad, and M. Potthoff, Dynamical mean-field study of partial kondo screening in the periodic anderson model on the triangular lattice, *Phys. Rev. B* **92**, 235131 (2015).
- [21] R. Peters and N. Kawakami, Competition of striped magnetic order and partial Kondo screened state in the Kondo lattice model, *Phys. Rev. B* **96**, 115158 (2017).
- [22] T. Sato, F. F. Assaad, and T. Grover, Quantum Monte Carlo Simulation of Frustrated Kondo Lattice Models, *Phys. Rev. Lett.* **120**, 107201 (2018).
- [23] R. Islam, R. Ma, P. M. Preiss, M. Eric Tai, A. Lukin, M. Rispoli, and M. Greiner, Measuring entanglement entropy in a quantum many-body system, *Nature (London)* **528**, 77 (2015).
- [24] A. V. Gorshkov, M. Hermele, V. Gurarie, C. Xu, P. S. Julienne, J. Ye, P. Zoller, E. Demler, M. D. Lukin, and A. M. Rey, Two-orbital $\text{SU}(N)$ magnetism with ultracold alkaline-earth atoms, *Nat. Phys.* **6**, 289 (2010).
- [25] M. Dalmonte, B. Vermersch, and P. Zoller, Quantum simulation and spectroscopy of entanglement Hamiltonians, *Nat. Phys.* **14**, 827 (2018).
- [26] F. Parisen Toldin and F. F. Assaad, Entanglement Hamiltonian of interacting fermionic models, *Phys. Rev. Lett.* **121**, 200602 (2018).
- [27] T. Grover, Entanglement of interacting fermions in quantum monte carlo calculations, *Phys. Rev. Lett.* **111**, 130402 (2013).
- [28] A. H. Castro Neto, F. Guinea, N. M. R. Peres, K. S. Novoselov, and A. K. Geim, The electronic properties of graphene, *Rev. Mod. Phys.* **81**, 109 (2009).
- [29] J. Eisert, M. Cramer, and M. B. Plenio, Colloquium: Area laws for the entanglement entropy, *Rev. Mod. Phys.* **82**, 277 (2010).
- [30] M. Ohya and D. Petz, *Quantum Entropy and Its Use*, Theoretical and Mathematical Physics (Springer, Berlin, 2004).
- [31] R. Blankenbecler, D. J. Scalapino, and R. L. Sugar, Monte carlo calculations of coupled boson-fermion systems. *Phys. Rev. D* **24**, 2278 (1981).
- [32] S. R. White, D. J. Scalapino, R. L. Sugar, E. Y. Loh, J. E. Gubernatis, and R. T. Scalettar, Numerical study of the two-dimensional hubbard model, *Phys. Rev. B* **40**, 506 (1989).
- [33] F. F. Assaad and H. Evertz, World-line and Determinantal Quantum Monte Carlo Methods for Spins, Phonons and Electrons, in *Computational Many-Particle Physics*, Lecture Notes in Physics, Vol. 739, edited by H. Fehske, R. Schneider, and A. Weiße (Springer, Berlin, 2008) pp. 277–356.
- [34] Z. Wang, F. F. Assaad, and F. Parisen Toldin, Finite-size effects in canonical and grand-canonical quantum Monte Carlo simulations for fermions, *Phys. Rev. E* **96**, 042131 (2017).
- [35] M. Bercx, F. Goth, J. S. Hofmann, and F. F. Assaad, The ALF (Algorithms for Lattice Fermions) project release 1.0. Documentation for the auxiliary field quantum Monte Carlo code, *SciPost Phys.* **3**, 013 (2017).
- [36] F. F. Assaad, T. C. Lang, and F. Parisen Toldin, Entanglement spectra of interacting fermions in quantum Monte Carlo simulations, *Phys. Rev. B* **89**, 125121 (2014).
- [37] C.-C. Chang, R. R. P. Singh, and R. T. Scalettar, Entanglement properties of the antiferromagnetic-singlet transition in the Hubbard model on bilayer square lattices, *Phys. Rev. B* **90**, 155113 (2014).
- [38] J. E. Drut and W. J. Porter, Hybrid Monte Carlo approach to the entanglement entropy of interacting fermions, *Phys. Rev. B* **92**, 125126 (2015).

- [39] J. E. Drut and W. J. Porter, Entanglement, noise, and the cumulant expansion, *Phys. Rev. E* **93**, 043301 (2016).
- [40] F. Parisen Toldin and F. F. Assaad, Entanglement studies of interacting fermionic models, *J. Phys.: Conf. Ser.* **1163**, 012056 (2019).
- [41] D. Blankschtein, M. Ma, A. N. Berker, G. S. Grest, and C. M. Soukoulis, Orderings of a stacked frustrated triangular system in three dimensions, *Phys. Rev. B* **29**, 5250 (1984).
- [42] R. Moessner and S. L. Sondhi, Ising models of quantum frustration, *Phys. Rev. B* **63**, 224401 (2001).
- [43] P. Broecker, F. F. Assaad, and S. Trebst, Quantum phase recognition via unsupervised machine learning, [arXiv:1707.00663](https://arxiv.org/abs/1707.00663).
- [44] J. S. Hofmann, F. F. Assaad, and T. Grover, Kondo Breakdown via Fractionalization in a Frustrated Kondo Lattice Model, [arXiv:1807.08202](https://arxiv.org/abs/1807.08202).